JOURNAL OF SOLID STATE CHEMISTRY **137,** 332–345 (1998)
ARTICLE NO. SC977746

Modeling the Thermal Decomposition of Solids on the Basis of Lattice Energy Changes

Part 1: Alkaline–Earth Carbonates

Annemarie de La Croix, Robin B. English,† and Michael E. Brown[1]

Chemistry Department, Rhodes University, Grahamstown, 6140 South Africa
E-mail: chmb@warthog.ru.ac.za

and

Leslie Glasser

Centre for Molecular Design, Chemistry Department, University of the Witwatersrand, P O Wits, 2050 South Africa
E-mail: glasser@aurum.chem.wits.ac.za

Received July 22, 1997; in revised form December 21, 1997; accepted December 30, 1997

Decompositions of many solids are of the form:

$$A(s) \rightarrow B(s) + \text{gases.}$$

As real examples of this reaction pattern, the decompositions of some alkaline-earth metal (Ca, Sr, Ba) carbonates

$$MCO_3(s) \rightarrow MO(s) + CO_2(g)$$

were selected for modeling. The crystal structures the reactants and the solid product oxides have been reported in the literature. Symmetry-controlled routes for transforming the reactant into the solid product oxide were devised as possible decomposition pathways. Lattice energies of the reactants, the conjectured transient intermediate structures, and the final products were then estimated by crystal modeling procedures, and profiles of energy changes during the proposed decomposition routes were constructed. Barriers in these energy profiles are compared with experimental values reported for the activation energies of the thermal decompositions. © 1998 Academic Press

INTRODUCTION

The processes which occur during solid decompositions are complex, leading to experimental observations which can be very different under even slightly changed conditions. These problems arise from the great variety of possibly uncontrolled system variables, such as the nature of the solid reactant (single crystal, powder), its pretreatment (grinding, annealing, etc., which influence the defect content and its nature), sample mass or size (which affect mass and energy transfer), and experimental conditions (temperature, rate of temperature rise, pressure, nature of the surrounding atmosphere, removal or otherwise of evolved gases, and so forth) (1).

Consequently, decomposition processes occur along different microscopic (molecular and atomic) paths, depending on the sample history and local conditions, such as chemical composition and crystal structure. The energetics of the processes will also differ as one compares conditions within the bulk of the crystal, on a planar surface, at a crystal corner or protuberance, along a grain boundary, adjacent to a dislocation, and within fine cracks.

In experimental terms, decompositions are studied by low-resolution bulk measurements such as changes in mass of a sample, or accumulated pressure of gas evolved from the sample. Such measurements average out the detailed behavior which occurs at the microscopic level. The microscopic behavior can only be revealed, to some extent, by repeated measurements with altered sample histories. A very few experimental measurements have been performed on complex decompositions in such a way as to attempt to isolate all but a few of the experimental variables. An example is work by Powell and Searcy (2) who examined the evolution of gases in vacuum from selected crystal faces of carbonates.

Given this exceedingly complex relation between observation and interpretation, it becomes worthwhile to attempt

† Deceased.
[1] To whom correspondence should be addressed.

0022-4596/98 $25.00

some kind of theoretical evaluation of the processes involved, in order to provide a fundamental basis for discussion and understanding. Such theoretical consideration can be undertaken at various levels of theory and for various kinds of decomposition processes. We report here on a first (and admittedly crude) attempt to tackle this problem at root.

The particular problem we have chosen is that of the thermal decompositions of simple ionic solids with complex anions, which produce a solid oxide and a simple gas, namely carbonate decomposition

$$MCO_3(s) \rightarrow MO(s) + CO_2(g),$$

where M is an alkaline–earth metal (Ca, Sr, Ba), and the corresponding peroxide decompositions (3):

$$MO_2(s) \rightarrow MO(s) + \tfrac{1}{2}O_2(g).$$

These have been chosen as initial examples because they are much studied but detailed mechanisms are still debated. For example, experimental activation energies for the decomposition of calcite ($CaCO_3$) range from 140 to 1600 kJ mol^{-1}. Carefully controlled experiments under well defined conditions (single crystal, vacuum) lead to a value of about 200 kJ mol^{-1}.

There are many choices available for attack by a theoretical method. The most fundamental approach would be to use quantum methods to examine the detailed chemical processes which might occur at a reconstructing crystal face as the decomposition proceeds. This approach may be discarded at once as impractical for systems of complex ions because full quantum methods, together with current computer power, are insufficient to handle problems of such magnitude (involving, as they do, extended lattice interactions). The next level—which is now just becoming accessible—is a treatment of a relaxing crystal surface using empirical force fields to model the interactions and changes. However, such force-field methods can hardly tackle a chemical transformation of the kind we contemplate.

Instead, we have chosen to follow a very crude path, which is computationally accessible but not experimentally very realistic to the decomposition; that is, we attempt to establish a thermodynamic path through the decomposition process. This may be compared with a Born-Haber calculation of lattice energy, which proceeds via improbable steps, but yields the overall energetics of the process. However, in contrast to the Born-Haber analysis, our procedure does not yield an exact result; rather, we examine a few simple conjectured paths for the processes and evaluate the energetic consequences thereof, and their accord (or otherwise) with bulk experiment. In this way, we provide a very first theoretical step toward a description of the experimental observations. Conjectured paths which do not accord with observations may then be discarded or amplified; those paths that do accord may give some insight into possible mechanisms, but no more than that. Nevertheless, this method has the significant effect of allowing us to place conjectured mechanisms in either of two opposing classes: those mechanisms which yield an activation energy greater than the experimental, and so are feasible even if not necessarily realistic; and those mechanisms with an activation energy lower then the experimental, which are thereby shown to be kinetically inaccessible and must be rejected. This is not unlike the procedure in the development of mechanisms of homogeneous reactions, where the proposed mechanism must fit the experimental kinetic observations, but is not thereby proven.

METHODOLOGY

We have chosen to examine changes in lattice energy over postulated paths from one defined crystal structure to another as the reactant system decomposes to product, releasing a gas in the process; thus, in our calculations, we deal with bulk materials of defined composition and structure. We do not consider the mechanism of conversion of one species or structure to another, nor the process of gas release from the bulk solid. This does not, however, imply that we regard the crystal as converting as a whole from structure to structure. Rather, our analysis simply requires that a given portion of sample (which could simply be composed of a few unit cells at a time) converts from one defined structure to another defined structure, for which we evaluate the energetics but ignore the path; in the final analysis, however, each portion of the sample must go through this same change. We do not allow for relaxation of structures from the defined ideal, such as might occur in the presence of defects of various kinds. However, there is evidence that reconstructions of this kind are not all-pervasive; for example, major surface reconstructions expected in some oxides in the absence of water vapor are actually avoided in the presence of water vapor, which thus seems to stabilize the surface in nearly its bulk form (4). Whether this might also occur in the presence of free $CO_2(g)$ is, of course, as yet unknown but might repay study.

LATTICE ENERGY CALCULATIONS

The lattice energy, W, of an ionic solid is defined as the energy which has to be supplied to separate one mole of the species from initial crystal lattice positions to infinite separation.

There are two principal aspects to the energy calculation: firstly developing a potential model (or force field) for the perfect lattice and, secondly, evaluating the parameters of

the potential model. The Buckingham potential:

$$\phi(r) = A \exp(-r/\rho) - (C/r^6)$$

(where r is the distance between interacting sites and A, ρ, and C are potential parameters), has been successful in modeling ionic materials in numerous studies (5–8) and has become the favored choice. Hence, the standard potential model used to calculate the lattice energy of perfect, ionic, and semi-ionic materials, including the Coulombic term, is:

$$W = \sum_{ij} \frac{q_i q_j}{r_{ij}} + \sum_{ij} A_{ij} e^{-r_{ij}/\rho_{ij}} - \sum_{ij} \frac{C_{ij}}{r_{ij}^6}.$$

Coulombic repulsion van der Waals

The rigid ion (point–charge) model has been used successfully to compute lattice energies of simple salts containing spherical ions, e.g., NaCl, CaF_2, CsCl, etc. (9). For lattices containing nonspherical complex ions, the simple point–charge model performs poorly and has had to be modified. A revised model, the rigid body model, described by Busing (10), treats the complex ion as a collection of discrete atoms which are themselves regarded as "point–charged" spheres. The "rigid body" is then assigned the formal charge of the complex, q_f, which is constrained by giving partial charges to the constituent atoms such that

$$\sum n_i q_i = q_r,$$

where q_i are the partial charges and n_i the number of constituent atoms, i. For the carbonate ion (CO_3^{2-}):

$$q_C + 3q_O = -2,$$

where q_C, q_O are the point charges assigned to the carbon and oxygen atoms, respectively. The partial charges, q_i, are fitted—like the short-range potential parameters—to the structural properties.

Allowance may be made for interatomic interactions within the rigid body. More recent work (8) uses models of complex ions which allow flexing of the ion, and include what Catlow *et al.* (11) describe as 3-body terms, e.g., angle-bending in CO_3^{2-}.

DETERMINATION OF INTERATOMIC POTENTIALS

The procedure for fitting potential parameters to experimental data (known as "optimization" of the potential) involves selecting a set of starting parameters (i.e., A_{ij}, ρ_{ij}, C_{ij}, q_i), to compute the lattice energy using an appropriate analytical potential function, as discussed above. The potential parameters are then adjusted in a least-squares-fitting routine until the best agreement between calculated and experimental crystal properties is achieved. Crystal properties typically used as observables are: crystal structure, relative permittivities, elastic constants, and phonon dispersion curves, if available. Lattice energies, determined from the Born-Haber cycle, have also been included by some workers (12), but they are not extensively used due to their variable reliability.

The assumption that a set of potential parameters is transferable from the crystal for which it was derived to another crystal environment relies on the fact that the environment does not appreciably affect the potentials (13). This is not always so, since interatomic potentials derived from fitting to the crystal properties contain, at a basic level, inherent physical properties of the atoms involved. Where "transferred" potential parameters perform poorly, Bush *et al.* (7) have pointed out that there is no way of determining whether the failure of the transferred parameters is due to the parameters being inappropriate to the changed chemical environment, or to shortcomings in the potential model employed. There is, however, substantial evidence to support the transferability of potential parameters (14, 15). Interatomic potentials fitted to multiple structure models (i.e., where a series of compounds is optimized concurrently) generate parameters that are intrinsically transferable within the series (7, 13).

In general, the number of observables (i.e., experimental crystal properties used in the fitting procedure) must be greater than or equal to the number of variables (i.e., adjustable parameters A_{ij}, ρ_{ij}, C_{ij}, and q_i for each interatomic interaction). To increase the number of observables, two strategies have been adopted in the present work: (i) The number of crystals with common features involved in the fitting is increased (e.g., MgO is added to the group CaO, SrO, and BaO). This procedure compromises the reliability of the parameters for a particular compound, but enhances the transferability of the parameters among a number of systems (6). (ii) The crystal structure is relaxed to that of a triclinic system, with no symmetry constraints applied. This strategy satisfies the formal requirement for a statistical fit but does not, in fact, provide more parameters that are essentially independent. Thus, the result of such a relaxed fitting process provides a feasible solution in a least-squares sense; other starting points will simply provide other feasible solutions.

SOFTWARE

The FORTRAN program WMIN by Busing (10) was used to optimize short-range potentials and perform the energy calculations and minimizations. This has been described in more detail elsewhere (9).

STRUCTURAL INFORMATION

The Alkaline–Earth Metal Oxides

The accuracy of lattice energy calculations depends on the quality of the crystal data used as reference. The crystal structures (16–19) of MgO, CaO, SrO, and BaO belong to the face-centered cubic system. Crystal data are given in Table 1. The density ratio (expt/calc) was used as a guide for assessing the accuracy of the structural data (see Table 1). The large discrepancies for SrO and BaO suggest possible experimental difficulties in measuring the densities.

The Alkaline–Earth Metal Carbonates

Calcium carbonate crystallizes naturally as calcite, aragonite, or vaterite. The calcite and aragonite structures are very similar and only slight alterations to the packing are needed to convert between them. The CO_3^{2-} group is planar in the calcite structures ($MgCO_3$, $CaCO_3$) and slightly nonplanar in the aragonite structures ($CaCO_3$, $SrCO_3$, $BaCO_3$).

The calcite structures (trigonal system, space group 167, $R\bar{3}c$) can be defined in terms of either hexagonal or rhombohedral axes. For comparison with the cubic oxides, the rhombohedral unit cell with its single axial length was preferred. The crystal data (21) are listed in Table 2.

The crystal structures of $CaCO_3$ (aragonite), $SrCO_3$, and $BaCO_3$ (22) belong to the orthorhombic system, space group 62, defined in terms of a nonstandard setting, *Pmcn*, with a tetramolecular unit cell, $Z = 4$. Data are included in Table 2.

The crystal structure of $CaCO_3$ (vaterite) (23, 24) has space group 194, $P6_3/mmc$. Data are included in Table 2 for completeness.

INTERATOMIC POTENTIAL PARAMETERS (A_{ij}, ρ_{ij}, c_{ij})

A different potential model and the corresponding values of the short-range interatomic potential parameters (A_{ij}, ρ_{ij}, C_{ij}) have been reported for the oxides MgO, CaO, SrO, and BaO (7, 25, 26). These could not be used in this study however, because of the differing models.

In deriving our short-range potential parameters, the following assumptions (proposed by Catlow *et al.* (26) and Sangster and Stoneham (25) were used: (a) the oxygen–oxygen interactions were taken to be the same in all the crystals where the oxidation states are equivalent, i.e., O^{2-}–O^{2-} in the oxides; (b) cation–cation interactions were assumed to be purely Coulombic; and (c) the anion–cation interactions were represented by the Born-Mayer potential $\phi(r) = Ae^{-r/p}$, i.e., the attractive r^{-6} term was ignored. The small contribution of such terms to the short-range potential is incorporated by small modifications of the Born-Mayer parameters (A_{ij} and ρ_{ij}).

TABLE 1
Crystal Data for the Cubic Alkaline–Earth Metal Oxides (Space Group No. 225, $Fm\bar{3}m$, Number of Formula units, $Z = 4$)

	(Ref)	Lattice constants a (Å)	Experimental density (20) D_0 (g cm^{-3})	Density ratio (expt/calc)
MgO	(16)	4.217	3.58	1.00
CaO	(17)	4.795	3.35	0.99
SrO	(18)	5.1396	4.7	0.93
BaO	(19)	5.496	5.72	0.93

Oxides

Parameters for Mg, Ca, Sr, and Ba oxides were estimated by reference to the crystal structures (Table 1) and lattice energies calculated by Huggins and Sakamoto (27) (Table 3). As starting values for A_{ij}, ρ_{ij}, and C_{ij}, those reported by Sangster and Stoneham (23) (listed in Table 4) were used. An optimized set of parameters, OPT1, also shown in Table 4, was obtained. The value of the "fitting" factor from WMIN, RDWST = 0.02, was good. (RDWST is the square root of the sum, over all the substances, of the derivatives of the lattice energy with respect to each parameter, plus the squares of the differences between the observed and calculated data (28)).

A second optimization was performed, in which the cubic oxide structures were relaxed to those of the triclinic system, thus allowing all the cell dimensions to be used as apparently independent observables (but, actually, only yielding a feasible parameter set). The lattice energies were omitted as observables in this optimization. The value of RDWST (0.145×10^{-5}) was considerably improved. The second parameter set, OPT2 (Table 4) follows the same trend as the set reported by Sangster and Stoneham (25), namely, the A_{ij} values (for the M^{2+}–O^{2-} interactions) decrease as the cation size increases. Parameter set OPT2 was used for modeling the decompositions. The optimized parameter sets, OPT1 and OPT2, were then used to calculate the cell dimensions and lattice energies of the oxides (Table 5). The set OPT1 (in which the lattice energies were used as observables) yielded lattice energies closer to the observed values, i.e., with errors of at most 0.03%, while the lattice energies calculated with set OPT2 (in which lattice energies were excluded from the fitting) compare well with recently reported values, i.e., values generally fall between those calculated by Sangster and Stoneham (25) and Bush *et al.* (7) (see Table 3). The value for MgO approximates well that given by Bush *et al.* (7).

TABLE 2
Crystal Data for the Alkaline–Earth Carbonates

		Rhombohedral (obverse) calcite structures (space group $R\bar{3}c$)					
		a (Å)	α (deg)	Z	V (Å^3)	Experimental density D_0 (g cm^{-3})	Density ratio (expt/calc)
$MgCO_3$	(21)	5.6751	48.18	2	93.02	2.96	0.983
$CaCO_3$	(21)	6.3750	46.08	2	122.62	2.71	1.00
		Orthorhombic aragonite structures (space group *Pmcn*)					
		a (Å)	b (Å)	c (Å)	Z	V (Å^3)	D_0 (g cm^{-3})	Density ratio (expt/calc)
$CaCO_3$	(22)	4.961	7.967	5.740	4	226.91	2.93	1.00
$SrCO_3$	(22)	5.090	8.358	5.997	4	254.97	3.70	0.96
$BaCO_3$	(22)	5.313	8.896	6.428	4	303.81	4.43	1.03
		Hexagonal vaterite structure (space group $P6_3/mmc$)					
		a (Å)	b (Å)	c (Å)	Z	V (Å^3)	D_0 (g cm^{-3})	Density ratio (expt/calc)
$CaCO_3$	(23)	7.148	7.148	16.95	12[a]	749.98	2.6	0.98
	(24)	4.13	4.13	8.49	2	125.41		0.98

[a] Reference (23) gives 8, which appears to be an error.

Carbonates

The charge distribution in CO_3^{2-} has been extensively investigated, e.g., by Ladd (30, 31), Jenkins and Waddington (32), Jenkins *et al.* (33), Yuen *et al.* (34), and Pavese *et al.* (35). The values published by the various authors are very different. Discrepancies between two sets of results (31, 32) have been the subject of published correspondence (36). Pavese *et al.* (35) included bond-bending and torsional terms in the CO_3^{2-} group and the interatomic potentials were fitted to elastic and vibrational data. Their charge distributions ($q_C = 0.985$, $q_O = -0.995$ for calcite; and $q_C = 0.817$, $q_O = -0.939$ for aragonite) were used as fixed values in this study, where the carbonate ion is assumed to be rigid.

TABLE 3
A Comparison of the Lattice Energies (kJ mol^{-1}) Reported for the Alkaline–Earth Metal Oxides

Reference	MgO	CaO	SrO	BaO
Kapustinskii[a]	− 3865	− 3489	− 3250	− 3088
Therm. cycle[b]	− 3791	− 3401	− 3223	− 3054
1957: HS[c]	− 3795	− 3414	− 3217	− 3029
1980: SS[d]	− 3956	− 3473	− 3223	− 3001
1993: B[e]	− 3955	− 3509	− 3281	− 3132
1994: WMIN (OPT2)[f]	− 3968	− 3486	− 3240	− 3021

[a] Kapustinskii equation (29).
[b] Therm. cycle = lattice energy calculated from the thermochemical cycle (20).
[c] HS = Huggins and Sakamoto (27).
[d] SS = Sangster and Stoneham (25).
[e] B = Bush *et al.* (7).
[f] WMIN (OPT2) = lattice energies calculated using the optimized parameter set, OPT2.

The energy parameters for the calcite structures ($MgCO_3$, $CaCO_3$) and the aragonite stuctures ($CaCO_3$, $SrCO_3$, $BaCO_3$) were optimized separately. Since no values were available as starting values for the energy parameters for $MgCO_3$, $SrCO_3$, and $BaCO_3$, estimates of these parameters, on the basis of the $CaCO_3$ values, were made. Results are reported in Table 6.

The agreement between the calculated and experimental structures is good (Table 7) except for $BaCO_3$. The lattice energies are compared in Table 7 with the values calculated using the Kapustinskii equation (29).

In all the charge-distribution trials, the lattice energy for calcite was found to be higher than that for aragonite. Reported values for the enthalpy of transition for the calcite → aragonite transformation (37, 38) range between 0.21 and 4.88 kJ mol^{-1}. Both Jenkins *et al.* (33) and Yuen *et al.* (34) (see Table 9) found that aragonite had the higher lattice energy. Pavese *et al.* (35) did not report lattice energies. The calcite and aragonite structures were then optimized together, as was done by Yuen *et al.* (34). This

TABLE 4
Optimized Short-Range Potential Parameters (A_{ij}, ρ_{ij}, and C_{ij}) for Each Ion Pair Combination in the Oxides

Parameters	SS	OPT1 Cubic	OPT2 Symmetry-released
A_{ij} (kJ mol^{-1})			
O–O	219.64130×10^4	121.84850×10^4	803.80900×10^4
Mg–O	12.303077×10^4	3.34116×10^4	12.13607×10^4
Ca–O	11.37848×10^4	5.47833×10^4	11.17443×10^4
Sr–O	9.16704×10^4	7.09582×10^4	8.97697×10^4
Ba–O	7.54609×10^4	8.51326×10^4	7.56742×10^4
ρ_{ij} (Å)			
O–O	0.1490	0.0173	0.1733
Mg–O	0.3012	0.3824	0.3004
Ca–O	0.3401	0.3837	0.3391
Sr–O	0.3736	0.3875	0.3722
Ba–O	0.4084	0.3971	0.4049
C_{ij} (kJ mol^{-1} Å^6)			
O–O	19.654×10^2	19.5384×10^2	20.4964×10^2
RDWST	—	0.0198	0.145×10^{-5}

Notes. RDWST is the square root of the sum, over all the substances, of the derivatives of the lattice energy with respect to each parameter, plus the squares of the differences between the observed and calculated data (28). Values in column 1 are those reported by Sangster and Stoneham (SS) (25); values in columns 2 and 3 are optimized using WMIN.

TABLE 5
Cell Dimensions (a) and Lattice Energies (W) Calculated for the Alkaline–Earth Metal Oxides, Using Parameter Sets OPT1 and OPT2

	a (Å)	W (kJ mol^{-1})
MgO		
Kap.	4.2123	− 3865
Calc OPT1	4.2059	− 3795
Calc OPT2	4.2059	− 3968
CaO		
Kap.	4.795	− 3489
Calc OPT1	4.789	− 3415
Calc OPT2	4.791	− 3486
SrO		
Kap.	5.1396	− 3250
Calc OPT1	5.1346	− 3218
Calc OPT2	5.1328	− 3240
BaO		
Kap.	5.496	− 3088
Calc OPT1	5.493	− 3029
Calc OPT2	5.490	− 3020

Note. Kap. = Using the Kapustinskii equation (29).

parameter set (Table 8, OPT8), yielded lattice energies in the expected order, as shown in Table 9.

MODELING THE THERMAL DECOMPOSITION OF ALKALINE–EARTH METAL CARBONATES TO OXIDES

The changes in lattice energy during the thermal decomposition of alkaline–earth metal carbonates to their respective solid oxides and gaseous CO_2, i.e.,

$$MCO_3(s) \rightarrow MO(s) + CO_2(g)$$

were calculated by devising symmetry-controlled routes for transforming the reactant structure into the product structure. The polymorphism of the carbonates had to be taken into account.

The decompositions of calcite ($CaCO_3$) and the aragonite-structured carbonates ($CaCO_3$, $SrCO_3$, $BaCO_3$) were modeled separately on the basis that, on heating, the aragonite-structured carbonates undergo a phase transition to the calcite structures before decomposing (38).

Setting the Decomposition Pathways

The following assumptions were made in modeling a decomposition route: (1) The reactants are pure crystalline carbonates. (2) The final solid products are the corresponding pure crystalline oxides, cubic space group $Fm\bar{3}m$. (3) Reaction is assumed to occur via a series of solid intermediates with structures changing along a postulated symmetry route connecting the reactant structure to the product structure. (4) Parameters needed for calculating the lattice energies of intermediates are assumed to be transferable from the known structure to the intermediate of similar composition. Thus the parameter sets OPT1 or OPT2 were used for the oxides and OPT3–8 for the carbonates, as appropriate. (5) The crystal structures are assumed to be perfect, i.e., no allowance is made for the influence of any kind of defect on the lattice energy, even though defects are known to be important in the mechanisms of the decompositions of solids.

This last assumption is a major deviation from reality in the modeling. It is defended on the basis that we wish here to explore only the maximum energetics of the decomposition pathway. Should this prove useful, then more appropriate calculations can be undertaken. This point is taken up again in the final Discussion.

Setting the Decomposition Pathway for Calcite

Three symmetry-controlled routes, namely PATH I, PATH II, and PATH III, were investigated, all starting from the calcite structure 1 (space group $R\bar{3}c$, rhombohedral unit cell with $a = 6.3750$ Å, $\alpha = 46.08°$) and proceeding to CaO (cubic space group $Fm\bar{3}m$ (structure 5) with $a = 4.795$ Å).

TABLE 6
Optimized Short-Range Parameters (A_{ij}, ρ_{ij}, and C_{ij}) for the Alkaline–Earth Metal Carbonates

Parameters	OPT3	OPT4	OPT5
A_{ij} (kJ mol^{-1} × 10^5)			
O–O	6.46542	2.83041	4.73436
Mg–O	9.09465		
Ca–O	5.64031	8.92411	4.85630
Sr–O		6.69437	3.42068
Ba–O		0.18677	0.15159
ρ_{ij} (Å)			
O–O	0.2761	0.2828	0.2700
Mg–O	0.2193		
Ca–O	0.2595	0.2492	0.2600
Sr–O		0.2674	0.2838
Ba–O		0.4796	0.4898
C_{ij} (kJ mol^{-1} Å^6 × 10^4)			
O–O	1.73014	1.25212	0.78844
RDWST	1.85	14.1	51.4

Notes. OPT3: optimized parameter set for calcite isomorphous structures. OPT4: optimized parameter set for aragonite isomorphous structures. OPT5: optimized parameters set for the polymorphic calcite and aragonite structures (excluding $MgCO_3$). RDWST is the square root of the sum, over all the substances, of the derivatives of the lattice energy with respect to each parameter, plus the squares of the differences between the observed and calculated data (28). OPT3, OPT4, and OPT5 are the parameter sets optimized using the CO_3^{2-} charge distribution $q_C = 0.985$, $q_O = -0.995$ for calcite; and $q_C = 0.817$, $q_O = -0.939$ for aragonite (35).

Figure 1 outlines part of the decomposition route, i.e., to structure 4* (a common structure through which all three pathways pass), while Fig. 2 shows the complete route for PATH III.

PATH I: The calcite structure and dimensions are retained while CO_2 is removed by replacing each CO_3^{2-} with O^{2-} (structure 2a). The cell is then adjusted from rhombohedral to cubic by altering the rhombohedral angle from 46.08° to 90° (structure 3). The dimensions are then compressed from 6.3750 Å to those of the body-centred tetragonal cell, $a = c =$ 3.3905 Å, $b = 4.795$ Å (structure 4*). The cell is then redefined (without an energy change) to face-centered cubic (structure 4). Finally the oxide ions assume their final positions (structure 5).

PATH II: The rhombohedral unit cell of calcite is first adjusted to form a cubic structure (structure 2b) without change of lattice axial length. This is followed by removal of CO_2 (structure 3), and then compression of the sides as in PATH I (to structure 4*) and thence to CaO.

PATH III: The rhombohedral unit cell of calcite is converted to cubic and the axial length is compressed to 4.795 Å (structure 2c). This is followed by removal of CO_2 (structure 3c) and the same path to structures 4* and 5 is followed.

TABLE 7
Cell Dimensions, Volumes and Lattice Energies for the Alkaline–Earth Carbonates Using OPT3, OPT4, and the Kapustinskii Equation (29)

OPT3 (calcite structures)	a (Å)	α (deg)	V (Å^3)	W (kJ mol^{-1})
$MgCO_3$				
Lit.	5.6751	48.18	93.04	− 3180
Calc.	5.6752	48.18	93.04	− 3412
% error	0.00	0.00	0.00	7.3
Kap.				− 3282
$CaCO_3$				
Lit.	6.3750	46.08	122.63	− 2987
Calc.	6.3527	46.31	122.35	− 2986
% error	− 0.35	0.50	− 0.23	0.0
Kap.				− 3004

OPT4 (aragonite structures)	a (Å)	b (Å)	c (Å)	V (Å^3)	W (kJ mol^{-1})
$CaCO_3$					
Lit.	4.9614	7.9671	5.7404	226.91	− 2987
Calc.	4.9583	7.9843	5.7406	227.26	− 2964
% error	0.06	0.22	0.00	0.15	− 0.8
Kap.					− 3004
$SrCO_3$					
Lit.	5.090	8.358	5.997	254.97	− 2720
Calc.	5.090	8.312	6.023	254.82	− 2825
% error	0.00	0.55	0.07	− 0.06	3.9
Kap.					− 2824
$BaCO_3$					
Lit.	5.3126	8.9858	6.4284	303.81	− 2615
Calc.	5.3170	8.8182	6.5056	305.02	− 2439
% error	0.44	0.87	1.20	0.40	− 6.7
Kap					− 2700

Notes: OPT3: optimized parameter set for calcite isomorphous structures. OPT4: optimized parameter set for aragonite isomorphous structures.

Lattice energies calculated for structures 1 to 5 in the proposed decomposition routes (PATHS I, II, and III) are listed in Table 10. The lattice energy shows an initial increase relative to $CaCO_3$, followed by a steady decrease after the removal of CO_2.

The decomposition of calcium carbonate ($CaCO_3(s) \rightarrow CaO(s) + CO_2(g)$) is endothermic (20), with $\Delta H = 178$ kJ mol^{-1}. To relate the changes in lattice energy to the changes in energy associated with the decomposition of the calcium carbonate, corrections must be made for the removal of CO_2 from the lattice. From the definition of lattice energy, the processes under consideration are

$$CaCO_3(s) \rightarrow Ca^{2+}(g) + CO_3^{2-}(g) \quad \ldots \quad \Delta H_1 \qquad [1]$$

$$CaO(s) \rightarrow Ca^{2+}(g) + O^{2-}(g) \quad \ldots \quad \Delta H_2. \qquad [2]$$

TABLE 8
Optimized Parameters for $CaCO_3$ (Calcite and Aragonite)

	Calcite	Aragonite	OPT6	OPT7	OPT8
A_{ij} (kJ mol^{-1})					
O–O	1.50856×10^8	1.36704×10^8	6.32018×10^5	3.50641×10^5	4.54312×10^5
Ca–O	1.97144×10^5	1.80461×10^5	5.68909×10^5	8.34780×10^5	3.63866×10^5
C–O	1.39531×10^{13}	5.22287×10^{14}			
ρ_{ij} (Å)					
O–O	0.1366	0.2107	0.2754	0.2751	0.2632
Ca–O	0.2886	0.2892	0.2597	0.2490	0.2688
C–O	0.0458	0.0402			
C_{ij} (kJ mol^{-1} Å^6)					
O–O	3.3481×10^2	3.34815×10^2	1.75353×10^4	1.03669×10^4	0.55908×10^4
RDWST	unknown	unknown	0.84	0.15×10^{-4}	23.3

Notes. Values in columns 1 and 2 are those reported by Pavese *et al.* (35) for a flexible carbonate ion, while those in columns 3–5 are derived assuming a rigid carbonate ion. OPT6: optimized parameter set for calcite. OPT7: optimized parameter set for aragonite. OPT8: optimized parameter set for calcite and aragonite. RDWST is the square root of the sum, over all the substances, of the derivatives of the lattice energy with respect to each parameter, plus the squares of the differences between the observed and calculated data (28).

Lattice energies are formally calculated at 0 K, but crystal structure data refer to room temperature, so fitting is effectively at room temperature. Now, $\Delta H = \Delta U + p\Delta V \approx \Delta U + \Delta nRT$, where Δn (= 2 for reactions [1] and [2]) is the change in the number of gaseous molecules. Therefore, using $T = 298$ K, $\Delta nRT \approx 5$ kJ mol^{-1}. This is within the uncertainties of the lattice energy values, and so $\Delta H \approx \Delta U = -W$ for the formation of gaseous ions.

TABLE 9
Comparison of Experimental and Calculated Lattice Energies for $CaCO_3$ (Calcite and Aragonite)

W (kJ mol^{-1})	Calcite	Aragonite	ΔW (kJ mol^{-1})
Therm. cycle[a]	− 2810		
1976: J[b]	− 2814	− 2820	6
1978: Y[c]	− 3017	− 3046	29
1995: WMIN (OPT3, OPT4)[d]	− 2986	− 2964	− 22
1995: WMIN (OPT5)[e]	− 2907	− 2921	4
1995: WMIN (OPT6, OPT7)[e]	− 2987	− 2949	− 38
1995: WMIN (OPT8)[f]	− 2882	− 2890	8

[a] Therm. cycle (20).
[b] J = Jenkins *et al.* (33).
[c] Y = Yuen *et al.* (34).
[d] WMIN (OPT3, OPT4) = W calculated from parameters optimized over all the alkaline-earth carbonates.
[e] WMIN (OPT5), WMIN (OPT6, OPT7) = W calculated from parameters in which calcite and aragonite were optimized separately.
[f] WMIN (OPT8) = W calculated from parameters in which calcite and aragonite were optimized together.

$\Delta H_1 \approx -W(CaCO_3) = 2907$ kJ mol^{-1} and $\Delta H_2 \approx -W(CaO) = 3486$ kJ mol^{-1}. For reaction [1] − [2],

$$CaCO_3(s) \rightarrow CaO(s) + CO_3^{2-}(g) - O^{2-}(g)$$

$$\Delta H_3 = \Delta H_1 - \Delta H_2 = 2907 - 3486$$
$$= -579 \text{ kJ mol}^{-1} \quad \ldots \quad \Delta H_3. \qquad [3]$$

For decomposition,

$$CaCO_3(s) \rightarrow CaO(s) + CO_2(g) \quad \ldots \quad \Delta H_4, \qquad [4]$$

where ΔH_4 (from tables of standard thermodynamic data (34)) = 178 kJ mol^{-1}. Finally, [4] − [3] yields

$$CO_3^{2-}(s) \rightarrow CO_2(g) + O^{2-}(g) \quad \ldots \quad \Delta H_5, \qquad [5]$$

with $\Delta H_5 = \Delta H_4 - \Delta H_3 = 178 - (-579) = 757$ kJ mol^{-1}.

Reaction [5] represents the reaction that takes place on removal of CO_2 from the lattice and, therefore, the value of 757 kJ mol^{-1} must be added to those energies calculated from the lattice devoid of CO_2. These processes are summarized in Fig. 3.

The energies corrected for the removal of CO_2 ($W_{corrected}$) are shown in Table 10. From the changes in the corrected lattice energies with reference to structure 1 (ΔW_1) (also shown in Table 10), which are plotted against reaction course in Fig. 4, the activation energies for the decomposition routes, i.e., PATHS I, II, and III, were calculated to be 906, 906, and 460 kJ mol^{-1}, respectively.

The Decomposition Pathway for Aragonite, Strontianite, and Witherite

The symmetry-controlled transformations postulated for the decomposition of the aragonite structures were based on those of calcite, on the assumption that the aragonite → calcite phase transitions (38) precede decomposition. Modeling of the transition, although an interesting problem, was not attempted. PATH III (Figs. 1 and 2) was used to compare the behavior of $CaCO_3$, $SrCO_3$, and $BaCO_3$. The lattice dimensions of all the calculated structures (from structure 2 onward) were based more on the dimensions of the product oxide than on the reactant carbonate. The assumption is that, since the decomposition is endothermic, the structure of the activated complex would be more similar to that of the product oxide than that of the reactant carbonate (39). The proposed route for the aragonite is identical to that for calcite, and modifications made for $SrCO_3$ and $BaCO_3$ (involving the lattice dimension, *a*, *b*, and *c*) were based on the dimensions of the resultant oxide. Lattice energies calculated for the structures in the proposed decomposition route, PATH III, for aragonite, strontianite,

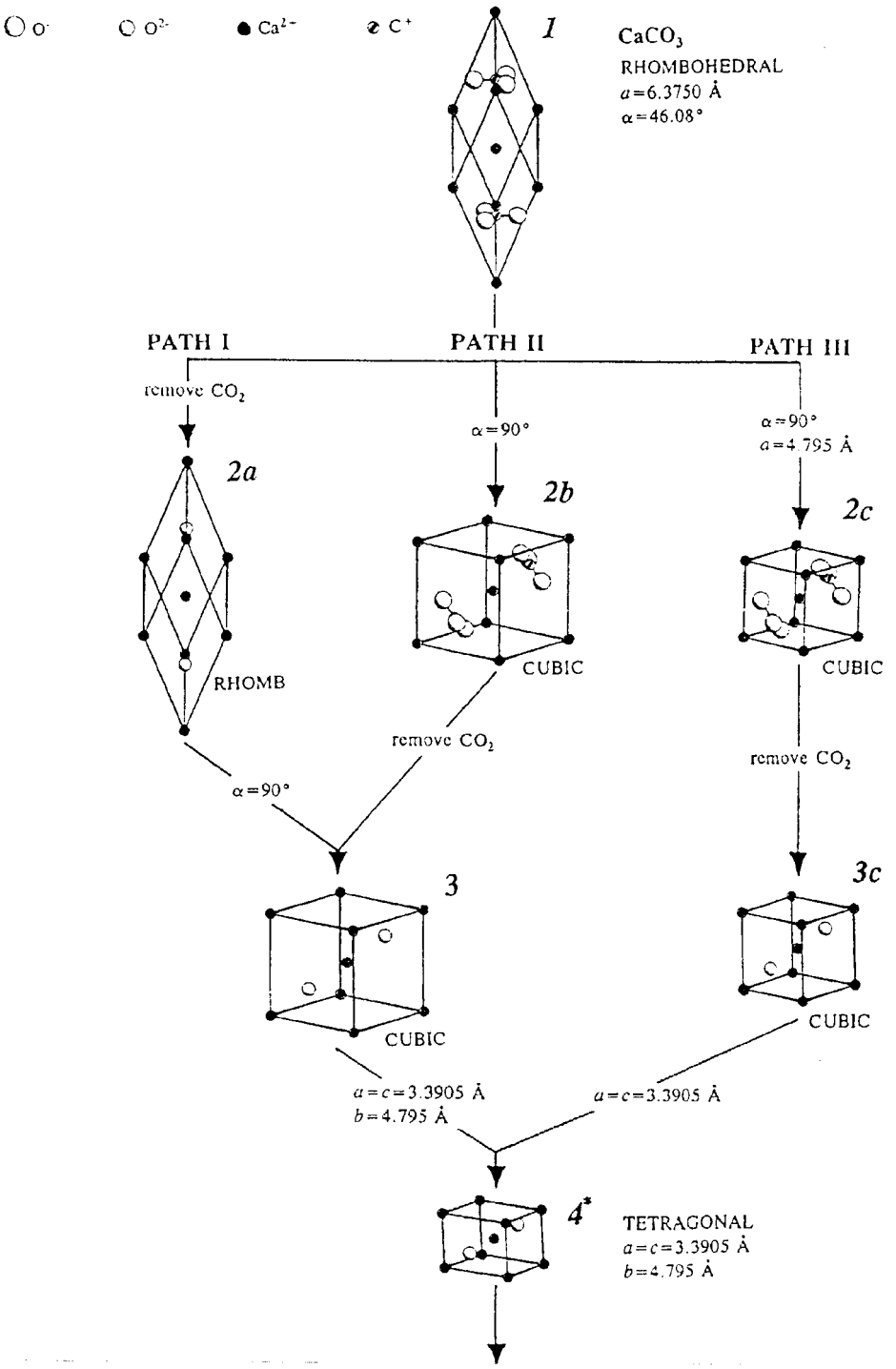

FIG. 1. Three postulated symmetry-controlled routes (PATH I, PATH II, PATH III) for the decomposition of $CaCO_3$ (calcite). Only part of the route is outlined, i.e., to structure 4* (a common structure through which all three pathways pass). See Fig. 2 for the complete route.

and witherite are listed in Table 11. The lattice energies corrected for the removal of CO_2 ($W_{corrected}$) and the changes in the corrected lattice energies with reference to the reactant (structure 1), ΔW_1, are also shown. The activation energies for aragonite, strontianite, and witherite were calculated to be 460, 524, and 580 kJ mol^{-1}, respectively.

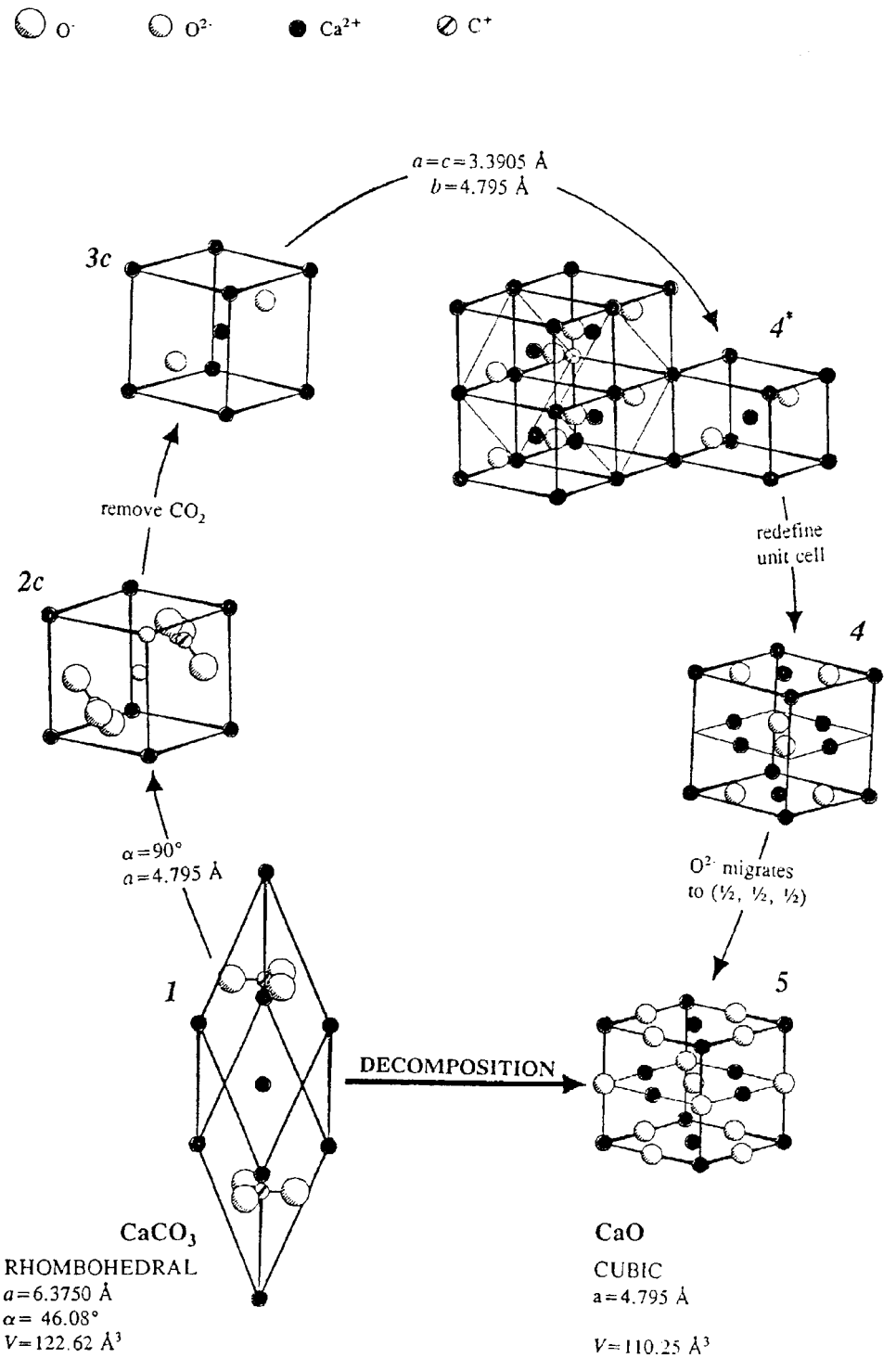

FIG 2. Postulated symmetry-controlled transformations (PATH III) for the decomposition of $CaCO_3$ to CaO.

Refined Symmetry-Controlled Route

On the assumption that the energy barrier would result from the removal of CO_2, i.e., the transition from structure 2c to 3c, the influence of removal of CO_2 was investigated. The lattice energies of the two postulated structures (i.e., before and after release of CO_2) are necessarily related to each other, since both structures have the same lattice

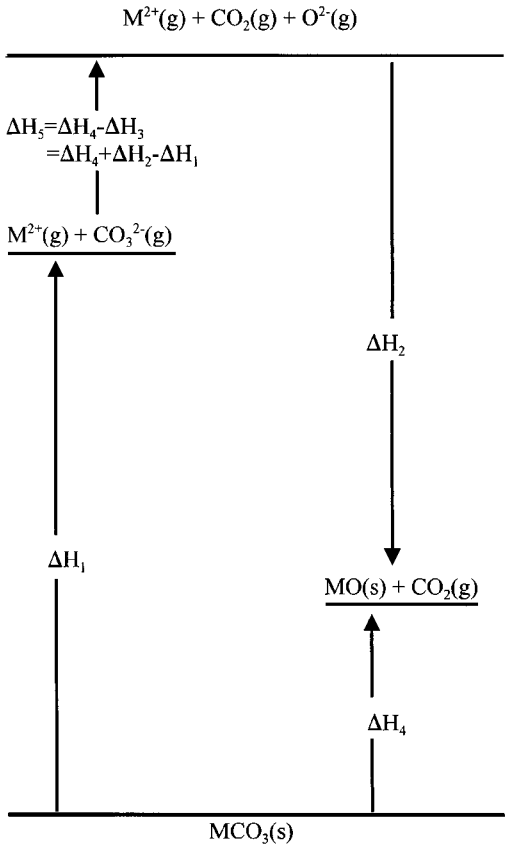

FIG. 3. The full energetic path: reactant to product via gaseous ions (not to scale.)

dimensions. To find the dimensions which would yield the lowest lattice energies for both 2c and 3c, the structures were compressed in stages starting from the dimensions of the product oxide, i.e., 4.795 Å, 4.795 Å, 5.1396 Å, and 5.496 Å for $CaCO_3$ (calcite and aragonite), $SrCO_3$, and $BaCO_3$, respectively. The lattice energy for structure 2c increases,

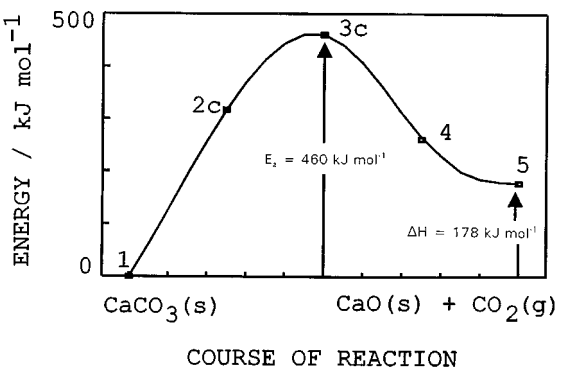

FIG. 4. Change in lattice energies (corrected for the removal of CO_2) with reference to the reactant structure (ΔW_1) plotted against course of the decomposition of calcite. Structure numbers indicated are from Table 10.

TABLE 10
Calculated Lattice Energies for the Structures in the Proposed Symmetry-Controlled Route for the Decomposition of Calcite

Structure	W (kJ mol^{-1})	$W_{corrected}$ (kJ mol^{-1})	ΔW_1 (kJ mol^{-1})
PATH I			
1	− 2907	− 2907	0
2a	− 2926	− 2169	738
3	− 2758	− 2001	906
4	− 3403	− 2646	261
5	− 3486	− 2729	178
PATH II			
1	− 2907	− 2907	0
2b	− 2357	− 2357	550
3	− 2758	− 2001	906
4	− 3403	− 2646	261
5	− 3486	− 2729	178
PATH III			
1	− 2907	− 2907	0
2c	− 2590	− 2590	317
3c	− 3204	− 2447	460
4	− 3403	− 2646	261
5	− 3486	− 2729	178

Notes. $W_{corrected} = W$ corrected for the removal of CO_2 and $\Delta W_1 =$ change in the corrected energies with reference to structure 1 ($CaCO_3$). $W_{corrected} = W - \Delta H_5 = W - 757$ kJ mol^{-1}.

TABLE 11
Calculated Lattice Energies (W) for the Postulated PATH III for the Decomposition of Aragonite, Strontianite and Witherite

Structure	W (kJ mol^{-1})	$W_{corrected}$ (kJ mol^{-1})	ΔW_1 (kJ mol^{-1})
$CaCO_3$ (aragonite)	($\Delta H_5 = 743$ kJ mol^{-1})		
1	− 2921	− 2921	0
2c	− 2590	− 2590	331
3c	− 3204	− 2461	460
4	− 3403	− 2660	261
5	− 3486	− 2743	178
$SrCO_3$ (strontianite)	($\Delta H_5 = 693$ kJ mol^{-1})		
1	− 2782	− 2782	0
2c	− 2502	− 2502	280
3c	− 2951	− 2258	524
4	− 3176	− 2483	299
5	− 3240	− 2547	235
$BaCO_3$ (witherite)	($\Delta H_5 = 856$ kJ mol^{-1})		
1	− 2431	− 2431	0
2c	− 2207	− 2207	224
3c	− 2707	− 1851	580
4	− 2969	− 2113	318
5	− 3020	− 2164	267

Notes. $W_{corrected} = W$ corrected for the removal of CO_2 and $\Delta W_1 =$ change in the corrected energies with reference to structure 1. $W_{corrected} = W - \Delta H_5$.

while that for structure 3c (removal of CO_2) decreases, as the initial unit cell dimensions are compressed, yielding lower E_a values. A contraction of approximately 5% in the initial unit cell dimensions decreases the overall E_a values to 422, 422, 465, and 499 kJ mol^{-1}, for $CaCO_3$ (calcite and aragonite), $SrCO_3$, and $BaCO_3$, respectively, (compared with 460, 460, 524, and 580 kJ mol^{-1}, respectively, for unrefined PATH III).

DISCUSSION AND CONCLUSIONS

Basic Assumption

In this study, the decompositions of some ionic carbonates:

$$MCO_3(s) \rightarrow MO(s) + CO_2(g)$$

have been modeled on the assumption that the course of decomposition may be influenced by the changes in lattice energy of the solids involved in the reaction. It is important to stress that this model need not represent the way in which decomposition actually does take place (if this can ever be completely known), but the consequences of this initial assumption have been explored. The justification for doing so is that experimental rate measurements must represent some averaging of a large number of different processes at the molecular level, as discussed above. These experimental rate measurements are used to calculate an *apparent* activation energy (by operational definition). There have been many interpretations proposed for the physical significance of the activation energy in solid state decompositions (40), and this study explores one further possibility: the influence of lattice energy changes during the course of reaction in a simple model with analogies to the Born-Haber cycle.

Lattice Energies

A key factor in determining lattice energies is the determination of accurate and transferable potentials. The reliability of the interatomic potentials was assessed by calculating crystal structures, densities, and lattice energies (which were not included in the fitting). The overall agreement between experimental and calculated values, except for the lattice energy of $BaCO_3$, provides support for the adequacy of the potential model used. The transferability of the potentials, however, was not assessed. Thus the extent to which the potentials are valid for interatomic separations, which differ considerably from those in the perfect lattice (i.e., for the proposed intermediate structures in the postulated decomposition routes), is not known, but potentials of the present form are probably transferable (13).

Decomposition Pathways

There are many ways in which the crystal structure of a reactant could be converted into a crystalline product while losing some gaseous constituents. In this study, it has been assumed that this conversion will occur while a relatively high degree of symmetry is retained, with the unit cell dimensions and angles adjusting in a regular fashion. The transition state (39) is by definition not a stable structure and, hence, the lattice energies were calculated on the basis of postulated ionic positions. These positions could not be allowed to relax since the result would be the initial or final state, depending on the constituents remaining at the stage of decomposition being considered. Quite clearly, none of these paths involving, as they do, arbitrarily defined intermediates with unrelaxed structures could be regarded as representing kinetic mechanisms, but they do provide potentially useful information on possible way-stations along the path from reactant structure to product structure.

Energetics

The energetics of this process are not simply represented by the sequence of lattice energies, since there is an intermediate change in chemical composition (from $CaCO_3$ to CaO) which must be allowed for, in a standard thermodynamic calculation. The full energetic path: reactant to product via gaseous ions is shown in Fig. 3.

Finally, then, we have an energy profile along the postulated path for the decomposition process (Fig. 4). This figure shows an energy profile for the path with the lowest maximum, which then represents the "activation energy, E_a" for the path. (The path with lowest maximum is chosen because the more energetic paths will be correspondingly unlikely.) As can be seen, E_a in this case is 460 kJ mol^{-1}, which is greater than the best experimental value (200 kJ mol^{-1}); this then is regarded as having yielded a feasible thermodynamic path.

Comparison with Experimental Studies

The aragonite → calcite transformation is described as a first-coordination reconstructive transformation (41), where first coordination bonds are broken and reformed, i.e., the coordination number of Ca^{2+} changes from 9 (in aragonite) to 6 (in calcite). A dislocation glide mechanism (42), whereby motion of a partial dislocation causes a shear of the Ca^{2+} sublattice, has been proposed. The kinetics of the aragonite-calcite transformation have been extensively studied (38, 42–51). The transition has a small, positive enthalpy change (ΔH_{tr} from 0.21 to 4.88 kJ mol^{-1}), but has a high activation energy (E_a from 160 to 750 kJ mol^{-1}). The thermodynamic and kinetic parameters for the transition are

sensitive to particle size, impurity content, and sample treatment, as shown by the wide range of values reported.

The kinetics of the thermal decomposition of $CaCO_3$ are well known to be dependent on many factors, for example, the nature of the solid reactant (single crystal, powder) its pretreatment (grinding, etc., which influence the defect content), the sample mass, and experimental conditions, i.e., the presence or absence of CO_2, temperature, pressure, etc. Experimental E_a values ranging from 140 to 1600 kJ mol^{-1} have been reported. The clearly defined experiments of Powell and Searcy (2), using single crystals of calcite decomposed in vacuum to remove any influence of heat transfer or product gas diffusion, yielded crystalline CaO and gave an E_a value of 205 ± 13 kJ mol^{-1}.

The activation energies predicted in this study for the decompositions of the carbonates, i.e., 422, 422, 465, and 499 kJ mol^{-1} for $CaCO_3$ (calcite), $CaCO_3$ (aragonite), $SrCO_3$, and $BaCO_3$, respectively, are within the wide range of reported experimental values, although higher than the more reliable values (2). Calvo *et al.* (52) reported values of 111 and 87 kJ mol^{-1} for calcite and aragonite, respectively, while Judd and Pope (53) reported 222 kJ mol^{-1} for $SrCO_3$ and 284 kJ mol^{-1} for $BaCO_3$. Both the presence of CO_2 and a decrease in sample mass produce an increase in the experimental values (54) of E_a. The presence of CO_2 is not taken into account in the present calculation based on lattice energies, where the total removal of CO_2 is, in effect, assumed. The reported influence of decreasing sample mass suggests that the E_a value obtained (422 kJ mol^{-1}) in the symmetry-controlled route could fit into the extrapolation pattern given by Gallagher and Johnson (54): 303 kJ mol^{-1} for a 1-μm particle, 378 kJ mol^{-1} for a 10 nm particle, and quite feasibly continuing to about 420 kJ mol^{-1} for a single unit cell (about 0.6 nm).

The standard enthalpy of decomposition of $CaCO_3$ is 178 kJ mol^{-1} at 298 K. In vacuum, decomposition occurs at a measurable rate at about 1100 K. Some of the activation energies reported lie below 178 kJ mol^{-1} at 298 K, or 170 kJ mol^{-1} at 1100 K. One of the fundamental problems in comparing values of E_a and ΔH is that the "mole" referred to may not be the same species. ΔH refers to a mole of *reactant*, while E_a refers to a mole of *activated complex*. In the decomposition of solids it is usually assumed, perhaps without justification, that the "activated complex" (whatever its interpretation) is derived from the unit of reactant.

Concluding Comment

If the role of defects is to provide a lower energy pathway for decomposition via some sort of cooperative mechanism analogous to the movement of a line dislocation through a crystal lattice, then it is reasonable to expect that the apparent energy barriers for the postulated highly symmetry-controlled routes will be higher than the observed experimental values. This has proved to be the case for the carbonate decomposition mechanisms under investigation here. An analogous study of the decompositions of alkaline–earth peroxides (3), which provided rather different results, is reported and discussed in Part 2.

REFERENCES

1. M. E. Brown, D. Dollimore, and A. K. Galwey, "Reactions in the Solid State," Comprehensive Chemical Kinetics, Vol. 22. Elsevier, Amsterdam, 1980.
2. E. K. Powell and A. W. Searcy, *Metall. Mater. Trans. B*, **11,** 427 (1980).
3. A. de La Croix, R. B. English, M. E. Brown, and L. Glasser, *J. Solid State Chem.* **137,** 346 (1998).
4. N. H. de Leeuw and S. C. Parker, *J. Chem. Soc., Faraday Trans.* **93,** 467 (1997).
5. S. C. Parker, *Solid State Ionics* **8,** 179, (1983).
6. S. C. Parker, E. T. Kelsey, P. M. Oliver, and J. O. Titiloye, *Faraday Discuss.* **95,** 75 (1993).
7. T. S. Bush, J. D. Gale, C. R. A. Catlow, and P. D. Battle, *J. Mater. Chem.* **4,** 831 (1994).
8. N. Allan, A. L. Rohl, D. H. Gay, C. R. A. Catlow, R. J. Davey, and W. C. Mackrodt, *Faraday Discuss.* **95,** 275 (1993).
9. G. Brink, L. Glasser, and R. C. Mboweni, *J. Phys. Chem.* **93,** 2927 (1989).
10. W. R. Busing, "WMIN: A computer program to model molecules and crystals in terms of potential energy functions," ORNL-5747. U.S., Oak Ridge National Laboratory, 1981. Revised version, March 1984.
11. C. R. A. Catlow, R. G.Bell, and J. D. Gale, *J. Mater. Chem.* **4,** 781 (1994).
12. G. Brink and L. Glasser, *J. Mol. Struct.* **244,** 277 (1991).
13. H. le Roux and L. Glasser, *J. Mater. Chem.* **7,** 843 (1997).
14. E. Clementi, G. Corongiu, and G. Ranghino, *J. Chem. Phys.* **74,** 578 (1981).
15. G. Brink and L. Glasser, *J. Phys. Chem.* **94,** 981 (1990).
16. S. Sasaki, K. Fujino, and Y. Takeuchi, *Proc. Jpn. Acad.* **55,** 43 (1979); *Chem. Abstr.* **90**:213591p.
17. G. Natta and L. Passerini, *Gazz. Chim. Ital.* **59,** 139 (1929); *Chem. Abstr.* **23**:4124.
18. W. Primak, H. Kaufman, and R. Ward, *J. Am. Chem. Soc.* **70,** 2043 (1948).
19. W. Gerlach, *Z. Phys.* **9,** 184 (1922); *Chem. Abstr.* **16**:2050.
20. R. C. Weast, Chief Ed., "Handbook of Chemistry and Physics," 73rd ed. CRC Press, Florida, 1992/3.
21. H. Effenberger, K. Mereiter, and J. Zemann, *Z. Kristallogr.* **156,** 233 (1981); *Chem. Abstr.* **95**:124504g.
22. J. P. R. de Villiers, *Am. Mineral.* **56,** 768 (1971).
23. H. J. Meyer, *Z. Kristallogr.* **128,** 183 (1969); *Chem. Abstr.* **71**:7547h.
24. S. R. Kamhi, *Acta Crystallogr.* **16,** 770 (1963).
25. M. J. L. Sangster and A. M. Stoneham, *Philos. Mag.* **43,** 597 (1981).
26. C. R. A. Catlow, W. C. Mackrodt, M. J. Norgett, and A. M. Stoneham, *Philos. Mag.* **35,** 177 (1977).
27. M. L. Huggins and Y. Sakamoto, *J. Phys. Soc. Japan* **12,** 241 (1957); *Chem. Abstr.* **51**:11802c.
28. A. de La Croix, MSc Thesis, Rhodes University, 1996.
29. A. F. Kapustinskii, *Z. Phys. Chem.* (Leipzig), **B22,** 257 (1933); *Chem. Abstr.* **27**:5227; *J. Phys. Chem.* (*USSR*), **5,** 59 (1934); *Chem. Abstr.* **28**:4955; *Acta Physicochim. URSS* **18,** 370 (1943); *Chem. Abstr.* **38**: 5705.
30. M. F. C. Ladd, *Trans. Faraday Soc.* **65,** 2712 (1969).

31. M. F. C. Ladd, *Theor. Chim. Acta*, **25,** 400 (1972).
32. H. D. B. Jenkins and T. C. Waddington, *Nature* (*London*), **232,** 5 (1971).
33. H. D. B. Jenkins, K. F. Pratt, B. T. Smith, and T. C. Waddington, *J. Inorg. Nucl. Chem.* **38,** 371 (1976).
34. P. S. Yuen, M. W. Lister, and S. C. Nyburg, *J. Chem. Phys.* **68,** 1937 (1978).
35. A. Pavese, M. Catti, G. D. Price, and R. A. Jackson, *Phys. Chem. Miner.* **19,** 80 (1992).
36. M. F. C. Ladd, *Nature* (*London*) **238,** 125 (1972); H. D. B. Jenkins and T. C. Waddington, *Nature* (*London*) **238,** 126 (1972).
37. F. D. Rossini, D. D. Wagman, W. H. Evans, S. Levine, and Irving Jaffe, Eds., "Selected Values of Chemical Thermodynamic Properties," Circular of the National Bureau of Standards 500. United States Government Printing Office, Washington, D.C., 1952.
38. C. N. R. Rao, "Crystal Structural Transitions in Inorganic Nitrites, Nitrates and Carbonates." National Bureau of Standards, Washington, D.C., 1975.
39. R. Shannon, *Trans. Faraday Soc.* **60,** 1902 (1964).
40. A. K. Galwey and M. E. Brown, *Proc. R. Soc. London Ser. A* **450,** 501 (1995).
41. C. N. R. Rao and K. J. Rao, "Progress in Solid State Chemistry," Vol. 4. Pergamon, Oxford, 1967.
42. M. Madon and P. Gillet, *Earth Planet. Sci. Lett.* **67,** 400 (1984).
43. N. S. Brar and H. H. Schloessin, *Can. J. Earth Sci.* **16,** 1402 (1979).
44. M. S. Rao, *Indian J. Chem.*, **11,** 280 (1973).
45. C. R. M. Rao and P. N. Mehrotra, *Can. J. Chem.* **56,** 32 (1978).
46. N. D. Topor, L. I. Tolokonnikova, and B. M. Kadenatsi, *J. Thermal Anal.* **20,** 169 (1981).
47. J. Morales, L. Hernan, L. V. Flores, and A. Ortega, *J. Thermal Anal.* **24,** 23 (1982).
48. J. Morales, L. Hernán, M. Macias, and A. Ortega, *J. Mater. Sci.* **18,** 2117 (1983).
49. J. Perić, R. Krstulović, T. Ferić, and M. Vučak, *Thermochim. Acta* **207,** 245 (1992).
50. M. Liu and R. A. Yund, *Contrib. Mineral. Petrol.* **114,** 465 (1993).
51. J. V. Dubrawski and B. M. England, *J. Thermal Anal.* **39,** 987 (1993).
52. E. G. Calvo, B. Aparicio, and A. R. Salvador, *Thermochim. Acta* **143,** 339 (1989).
53. M. D. Judd and M. I. Pope, *J. Thermal Anal.* **4,** 31 (1972).
54. P. K. Gallagher and D. W. Johnson, Jr., *Thermochim. Acta* **6,** 67 (1973).